

Exciton polaritons in semiconductor quantum microcavities in a high magnetic field

A. Armitage, T. A. Fisher, M. S. Skolnick, D. M. Whittaker,* and P. Kinsler
Department of Physics, University of Sheffield, Sheffield S3 7RH, United Kingdom

J. S. Roberts

Department of Electronic and Electrical Engineering, Sheffield S1 3JD, United Kingdom

(Received 15 November 1996; revised manuscript received 12 February 1997)

Exciton-photon polariton coupled mode spectra in (In)GaAs-GaAs-(Al)GaAs semiconductor quantum-microcavity structures are studied in magnetic fields up to 14 T. Very-well-resolved spectra are observed with large vacuum Rabi splittings of 7.1 meV being found due to the enhanced exciton oscillator strength in a high magnetic field. The spectra exhibit strong circular polarization with marked Zeeman splitting observed between the σ^+ and σ^- polarizations. Temperature tuning is employed to vary the exciton ($|c_e|^2$) and cavity ($|c_l|^2$) fractions of the polariton modes throughout the resonance regime. $|c_e|^2$ and $|c_l|^2$ are deduced as a function of detuning, from fitting of the observed peak positions as a function of temperature to a two-level coupled-mode model. The two-level model is found to explain the variation of Zeeman splitting with detuning very well, with the on-resonance Zeeman splitting being one half of the unperturbed exciton splitting. Anomalous narrowing of the lower polariton branch is found through the resonance regime. The observations are found to be in good agreement with a motional narrowing model for the polariton linewidths. The Zeeman splittings are investigated as a function of In composition in the quantum wells. Reasonable agreement with literature values for bare quantum wells is found, with a sign reversal of the polarization for GaAs relative to $\text{In}_x\text{Ga}_{1-x}\text{As}$ quantum wells being observed. Finally, coupling of the cavity mode to exciton excited states corresponding to higher Landau levels is seen, with vacuum Rabi splittings in good agreement with the results of exciton oscillator strength calculations. [S0163-1829(97)04124-6]

I. INTRODUCTION

There is very significant interest at the present time in the study of exciton-photon, polariton phenomena in semiconductor quantum microcavities (QMC's). One of the main reasons for this interest is the ability, in such structures, to control the properties of both excitons and photons, and the polariton coupling between them.¹ The excitonic properties are controlled by quantum wells (QW's) embedded in the cavity, while the photonic properties are determined by the Fabry-Pérot modes of the cavity. The coupling between the excitons and photons is termed vacuum Rabi coupling,¹ and leads to the formation of so-called cavity polaritons.²

Magnetic fields have been shown recently to provide a valuable probe of the properties of the coupled polariton states in such microcavities.³⁻⁵ In our previous work, we investigated the effect of the magnetic-field-induced increase of exciton oscillator strength and Zeeman splitting on the vacuum Rabi coupling.⁴ These results show that the vacuum Rabi splitting increases with magnetic field, as expected from the predicted increase in exciton oscillator strength due to shrinkage of the exciton wave function. This is in contrast to our electric-field tuning experiments which show a decrease in vacuum Rabi splitting on resonance as the electric field across the QW (Refs. 6 and 7) is increased. Transfer matrix reflectivity (TMR) simulations and circular polarization measurements were employed in Ref. 4 to show that the spin components of the exciton are fully decoupled, with each exciton spin component interacting with the appropriately circularly polarized component of the photon mode. In magnetic-field work by other authors, Tignon *et al.*³ report

tuning of the cavity mode through several higher-energy Landau levels and deduce the effects of increased exciton oscillator strength on the vacuum Rabi splitting from the study of spectra near resonance. Berger *et al.*⁵ report a study of the magnetic-field-induced increase in vacuum Rabi splitting and time-resolved Rabi oscillation frequency and compare their results to magnetoabsorption spectra from bare quantum wells not confined in microcavities.

In the present paper, we report the results of circularly polarized reflectivity measurements at high magnetic field (14 T) where the tuning of the exciton through the cavity mode is achieved by variation of temperature from 20 to 115 K. The observed spectra are of high quality with the upper and lower branches being very well resolved, with vacuum Rabi splitting of 7.1 meV and linewidths of ~ 1 meV. The results are fitted to a two-level coupling model between the exciton and cavity modes. The model is shown to account very well for the variations of the peak positions and the Zeeman splittings of the upper and lower polariton branches as a function of temperature. Resonance is shown to correspond to equal integrated areas of the two coupled-mode peaks. The observation of enhanced narrowing of the polariton linewidths in the resonance regime, first reported in Ref. 8 and ascribed to the occurrence of enhanced statistical averaging ("motional narrowing") over the quantum-well disorder potential in the resonance regime, is discussed. The important role of the high magnetic fields in these observations is described. We discuss the effect of the exciton Zeeman splitting on the polariton spectra in detail for a structure with $\text{In}_{0.13}\text{Ga}_{0.87}\text{As}$ QW's and compare this to that seen for microcavities with QW's of lower In composition of 6% and

0%. Finally, the coupling of the cavity mode to higher $N = 1$ excitonic Landau level states is described.

The paper is organized as follows. Section II describes the structures studied and the experimental techniques employed. The temperature tuning reflectivity measurements for both σ^+ and σ^- polarization are presented in Sec. III A. The coupled-mode behavior is analyzed and the exciton and cavity fractions of the polariton wave function deduced as a function of temperature and hence of exciton-cavity detuning. This is followed in Sec. III B by analysis and fitting of the Zeeman splitting of the upper and lower polariton branches to a two-level coupled-mode model. In Sec. IV the polariton linewidth behavior as a function of exciton-cavity detuning is presented, and interpreted in terms of the motional narrowing theory. In Sec. V the Zeeman splittings are analyzed further and results compared for samples containing quantum wells of different indium composition. Tuning of higher Landau-level states through the cavity mode is described in Sec. VI, and, finally, in Sec. VII the main conclusions are summarized.

II. EXPERIMENT

The principal QMC structure described in this paper consists of a λ GaAs cavity, sandwiched between two distributed Bragg reflectors (DBR's). The DBR's each consist of 20 periods of $\lambda/4$ layers of $\text{Al}_{0.13}\text{Ga}_{0.87}\text{As}$ and AlAs. Three $\text{In}_x\text{Ga}_{1-x}\text{As}$ ($x=0.13$) QW's are embedded centrally in the GaAs cavity at the antinode of the cavity photon mode. Since the QW is strained, only heavy-hole exciton transitions are observed. Results from this sample are also presented in Refs. 4 and 8. In addition to this sample magnetorefectivity spectra for samples of similar design but containing QW's of composition $x=0.06$ and 0 are also presented. The $x=0$ GaAs QW is embedded in a λ $\text{Al}_{0.2}\text{Ga}_{0.8}\text{As}$ cavity, surrounded by $\text{Al}_{0.46}\text{Ga}_{0.54}\text{As}/\text{AlAs}$ DBRs.⁶ All samples were grown by metal-organic vapor-phase epitaxy.

The samples are mounted in a 16 T Oxford Instruments superconducting magnet. The reflectivity spectra are obtained with illumination from an unpolarized white light source. The reflected light was analyzed into its circularly polarized components before being dispersed by SPEX single or double spectrometers and detected by a liquid-nitrogen-cooled Ge photodiode.

III. REFLECTIVITY MEASUREMENTS AT HIGH MAGNETIC FIELD

A. Temperature tuning experiments: Coupled-mode behavior

A series of reflectivity spectra at $B = 14$ T for the principal QMC sample ($x=0.13$) investigated is presented in Fig. 1, as a function of temperature from 20 to 115 K. Spectra are presented for both σ^+ and σ^- circular polarization (the full and dashed lines, respectively). The spectra are found to be strongly circularly polarized, with the σ^+ components lying at higher energy, corresponding to positive exciton g -values. We showed in Ref. 4 that the strong polarization of the spectra demonstrates that the two exciton spin components are fully decoupled, and that each interacts independently with the appropriate circularly polarized cavity mode. The σ^+ and σ^- features arise from transitions involving the

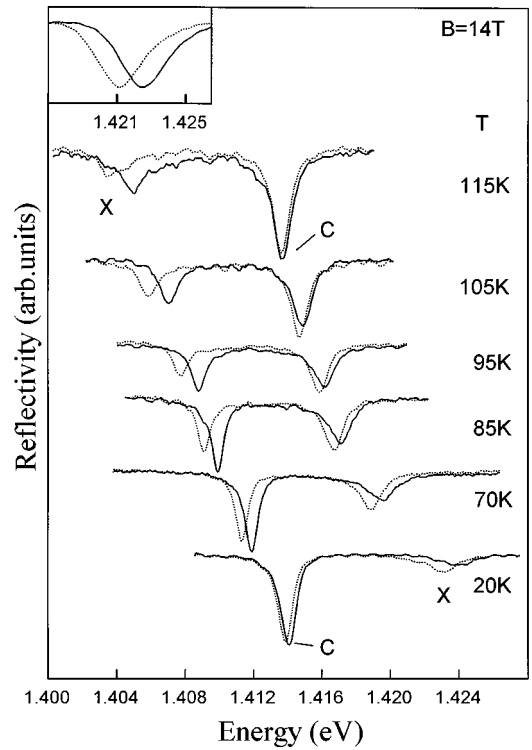


FIG. 1. Reflectivity spectra for quantum microcavity structure with $x=0.13$ at 14 T for σ^+ (full lines) and σ^- (dashed lines) circular polarizations as a function of temperature from 20 to 115 K. The mostly cavitylike features are labeled C and the mostly excitonlike features X. Resonance as defined by equal intensity for the upper and lower polariton features occurs at 70 K for σ^- and at 82 K for σ^+ . The upper inset shows σ^+ and σ^- reflectivity spectra for microcavity structure with top mirror etched off.

$m_j = +1$ and $m_j = -1$ spin angular momentum states of the exciton to the $J=0$ final state, as discussed in Sec. V.

At 20 K a strong, predominantly cavity feature is observed (labeled C) in both polarizations. The predominantly exciton feature (labeled X) is ~ 10 meV at higher energy and is of low intensity, as a result of the weak coupling to the cavity mode. Tuning of the exciton feature through the cavity mode is achieved by raising the temperature, the energy of the exciton state decreasing at a faster rate than that of the cavity mode, with no appreciable change in linewidth up to ~ 120 K.⁶ As the temperature is increased the strength of the excitonlike feature increases until on resonance there are two coupled polariton branches, each with equal exciton and photon components. The upper and lower polariton branches have equal integrated intensity at 70 K for the σ^- polarization and at 82 K for σ^+ , corresponding to resonance for the two polarizations. It should be noted that the upper polariton branch has a broader linewidth than the lower branch, as discussed further in Sec. IV. As a result, equal integrated area does not correspond to equal depth of the two features; on resonance the depth of the higher-energy feature is less than that of the lower-energy feature. As the temperature is increased further beyond resonance, the predominantly exciton feature moves further to lower energy and weakens in intensity as the mixing with the cavity mode decreases.

Characteristic anticrossing behavior between the two polariton components is also observed, as shown in the plot of

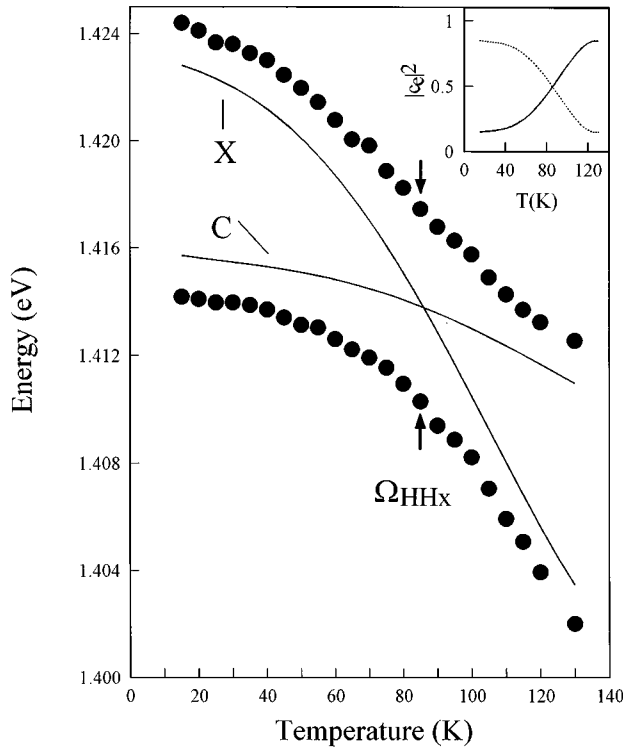


FIG. 2. Peak positions (filled circles) of the upper and lower polariton features as a function of temperature for σ^+ polarization. Ω_{HHx} indicates the on-resonance vacuum Rabi splitting ($=7.1$ meV). The unperturbed exciton and cavity variations deduced from the two-level coupling model are shown by the full lines, and are labeled X and C, respectively. The inset shows the variation of the exciton and cavity fractions ($|c_e|^2$, full line; $|c_l|^2$, dashed line) of the lower branch polariton wave function as a function of temperature deduced from the two-level model.

the energy positions of the σ^+ polariton features in Fig. 2. Similar anticrossings have been reported previously for exciton-cavity coupled modes in microcavities in measurements as a function of position by Weisbuch *et al.*,¹ and in temperature and electric-field tuning experiments by Fisher *et al.*^{6,7} The energy splitting on resonance Ω_{HHx} is the vacuum Rabi splitting. Its value on resonance of 7.1 meV is much greater than the linewidth of the individual components (0.8 and 1.5 meV, respectively,) and corresponds to the strong-coupling limit¹ between the two modes. As discussed in Refs. 1 and 3–6, Ω_{HHx} is approximately proportional to the square root of the exciton oscillator strength f . f is enhanced by a factor of ~ 2 between 0 and 14 T due to shrinkage of the exciton wave function, leading to enhancement of the vacuum Rabi splitting and the very-well-resolved spectra of Fig. 1.

We now fit the results of Figs. 1 and 2 to a coupled two-level exciton-photon model. The fitting enables the uncoupled exciton and cavity mode energy variations and the exciton and cavity photon fractions of the polariton wave functions to be deduced as a function of temperature. These results are then used in the analysis of the Zeeman splittings and linewidth variations as a function of temperature, and hence as a function of the detuning from the exciton-cavity resonance. A brief discussion of the two-level model was presented in Ref. 8.

Each polariton mixed mode wave function $|p\rangle$ can be written as a linear combination of the exciton and cavity photon mode components ($|e\rangle$ and $|l\rangle$, respectively), and is given by

$$|p\rangle = c_e|e\rangle + c_l|l\rangle. \quad (1)$$

Away from resonance, only the cavity feature (corresponding to $|c_l|^2 \rightarrow 1$, $|c_e|^2 \rightarrow 0$) gives rise to a significant feature in reflectivity; the excitonic feature ($|c_e|^2 \rightarrow 1$, $|c_l|^2 \rightarrow 0$) is unobservable since it arises within the high reflectivity region of the distributed Bragg reflectors. As resonance is approached, the mixing of the two wave functions increases and the characteristic exchange of intensity between two coupled modes is observed with $|c_e|^2 = |c_l|^2 = \frac{1}{2}$ corresponding to equal intensities on resonance.

From knowledge of the on-resonance splitting Ω_{HHx} (see Fig. 2) and the measured peak positions of Fig. 2 the unperturbed exciton and cavity positions can be obtained from solution of the eigenvalue equation obtained from diagonalization of the Hamiltonian for the two-level coupled system:

$$(H + V)|p\rangle = E|p\rangle, \quad (2)$$

where H is the unperturbed Hamiltonian and $V = \Omega_{\text{HHx}}/2$ is the coupling potential. The Hamiltonian for the two-level coupled system can be written in the basis of the uncoupled eigenfunctions as

$$\begin{pmatrix} \Delta/2 & \Omega_{\text{HHx}}/2 \\ \Omega_{\text{HHx}}/2 & -\Delta/2 \end{pmatrix},$$

where Δ is the energy separation (the detuning) between the unperturbed components. Diagonalizing this Hamiltonian gives the eigenvalues $\pm \frac{1}{2}(\Delta^2 + \Omega_{\text{HHx}}^2)^{1/2}$. The energy separation between the perturbed components is thus $\delta = (\Delta^2 + \Omega_{\text{HHx}}^2)^{1/2}$. Using the measured perturbed peak positions and Ω_{HHx} the minimum (on-resonance) peak separation as input parameters, the unperturbed exciton and cavity peak positions were then calculated and are shown by the full lines on Fig. 2. The deduced curves show the expected strong decrease of exciton (X) energy with temperature (~ 18 meV from 0 to 130 K) and the relatively weaker decrease in cavity (C) energy by ~ 4 meV over the same temperature range.⁶ The crossing point (resonance) between the two uncoupled modes is found to occur at 85 K in very good agreement with the resonance temperature of 82 K deduced above from the integrated intensities of the two branches.

The same diagonalization procedure also enables the c_e and c_l eigenvector parameters for each branch to be deduced as a function of temperature.⁹ The results are shown for the exciton and cavity fractions of the lower branch polariton wave function in the inset to Fig. 2. As expected, at low temperature $|c_e|^2$ is small and $|c_l|^2$ is large since the polariton feature is mainly cavitylike. At high temperature, $|c_e|^2$ is large and $|c_l|^2$ is small, again as expected since the lower branch is then mainly excitonlike. For the upper branch polariton, the variations of $|c_e|^2$ and $|c_l|^2$ with temperature (not shown) are reversed with $|c_e|^2$ tending to 1 and 0 at low and high temperature, respectively.

In this section we have used a simple two-level model to analyze the coupled mode behavior. In some of our previous

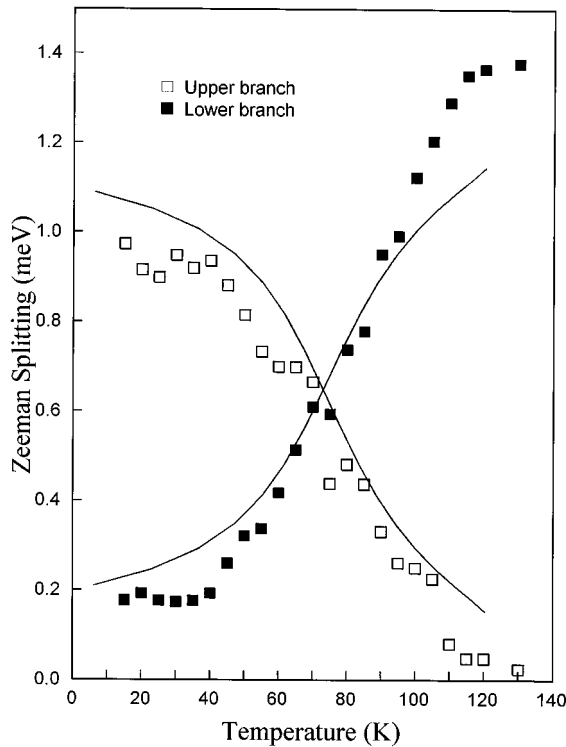


FIG. 3. Zeeman splitting between the σ^+ and σ^- circularly polarized components. Open squares, upper polariton branch; filled squares, lower branch. The full lines are the fit to the two-level model for equal Zeeman splittings at 75 K and an unperturbed exciton splitting of 1.4 meV.

publications^{4,7} we have analyzed the anticrossing phenomena using transfer matrix simulations of the structures. We have verified that identical results are obtained for the two approaches. However, the present approach has the advantage of enabling the exciton and cavity fractions of the polariton to be deduced in a very straightforward way.

B. Zeeman splitting as a function of a temperature

The measured polariton Zeeman splittings between the σ^+ and σ^- components for the upper branch (open squares) and lower branch (filled squares) are shown in Fig. 3 as a function of temperature. At 20 K, the upper branch which has a higher exciton component, has a Zeeman splitting of ~ 1 meV, whereas the lower branch has a splitting of only 0.2 meV since it is mostly cavitylike. The fact that it has a small splitting arises from weak mixing with the exciton mode, since the cavity mode itself is unaffected by magnetic field. Raising the temperature increases the exciton-photon mixing as discussed in Sec. III A. The observed Zeeman splitting on the upper branch thus decreases as the photon component increases. At the same time the Zeeman splitting on the lower branch increases as the exciton component increases. At $T=75$ K the Zeeman splittings for both the upper and lower branch are equal, corresponding to nearly equal exciton and photon components for the two branches.¹⁰ Raising the temperature beyond this value increases the exciton component of the lower branch and decreases that of the upper branch, until at $T=130$ K the two branches are only weakly perturbed. The lower branch, which is now mostly

excitonlike ($|c_e|^2=0.8$) has a Zeeman splitting of 1.4 meV, whereas the upper branch exhibits almost no splitting since it is mostly cavitylike.

The Zeeman splittings were also investigated in a control sample where the top mirror had been etched off. In that case the bare exciton Zeeman splitting is expected, unperturbed by interaction with the cavity mode. The results are shown in the inset to Fig. 1. A Zeeman splitting of 1.3 meV is found, in good agreement with the value of 1.4 meV for the lower branch polariton at 130 K thus confirming the strong exciton contribution to the polariton wave function at this temperature.

The results of Fig. 3 were fitted to the two-level coupling model of Sec. III A, with the unperturbed σ^+ and σ^- exciton components shifted relative to one another by the unperturbed Zeeman splitting of 1.3 meV. The Hamiltonian of Eq. (2) was diagonalized separately for the σ^+ and σ^- components, and the energy separation of the σ^+ and σ^- components of the upper and lower branches thus obtained. The calculated $\sigma^+-\sigma^-$ splittings are shown by the full lines on Fig. 3, and are seen to be in very reasonable agreement with experiment over the whole temperature range.

There is only a small change of Zeeman splitting with temperature up to 40 K. Physically this arises since the initial shift of exciton energy with temperature is small. Full detuning is only approached in the high-temperature region ($T \rightarrow 130$ K), and as a result it is in this region only that the observed Zeeman splitting tends towards that of the control sample with top mirror removed. Finally we note that at the temperature (75 K) of equal Zeeman splittings (the average of the on-resonance temperatures for σ^+ and σ^- polarizations of Sec. III A),¹⁰ the observed splitting is 0.6 meV. This is approximately one half of the unperturbed Zeeman splitting, as expected for coupled-mode states with near equal exciton-photon character.¹¹

IV. POLARITON LINEWIDTHS AS A FUNCTION OF EXCITON FRACTION: EVIDENCE FOR MOTIONAL NARROWING

In this section we describe the variation of the polariton linewidths from 20 to 130 K as the exciton and cavity fractions of the polariton wave function are varied from the nearly off-resonance case at 20 K through resonance at ~ 75 K, to nearly off-resonance again at 130 K. The results of Sec. III A for the variation of the exciton fraction $|c_e|^2$ of each branch with temperature are then employed to display the linewidth results as a function of $|c_e|^2$. These results are analyzed in terms of the ‘‘motional narrowing’’ theory for polariton linewidths in a microcavity. The full theoretical details of this model are presented in Ref. 8. In this section we concentrate on a fuller description of the experimental results, together with a discussion of the advantage gained by performing such experiments in high magnetic field.

The upper and lower branch polariton linewidths (full width at half maximum) as a function of temperature are presented in Fig. 4 for the σ^+ polarization (very similar results are obtained for the σ^- polarization). The lower branch results are given by the filled squares and the upper branch results are open squares. At low temperature, the predominantly exciton upper branch (X) has linewidth of ~ 2.3 meV, whilst the

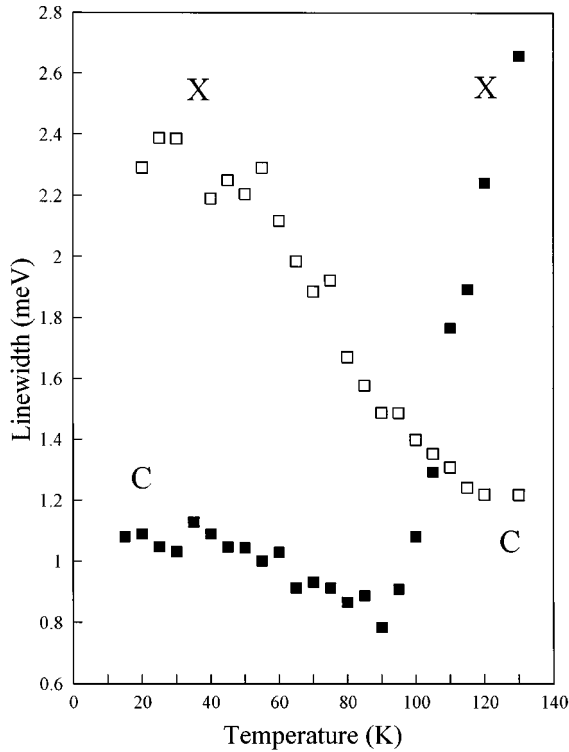


FIG. 4. Linewidths of polariton peaks as a function of temperature for σ^+ polarization. Open squares, upper branch; filled squares, lower branch.

predominantly cavity lower branch has narrower linewidth of ~ 1.1 meV. As temperature is increased and resonance is approached, *both* linewidths are observed to decrease, the upper branch strongly and the lower branch less rapidly, but still significantly. At resonance (85 K) the linewidths are 0.8 and 1.5 meV, respectively. As temperature is increased further the lower branch linewidth increases strongly as it becomes more excitonlike. The observed linewidth at 130 K is 2.7 meV, close to the linewidth observed from the bare QW in the structure with top mirror removed of 3.1 meV (Fig. 1 inset, solid line).

A more general way to examine the linewidth results is to plot them as a function of exciton fraction $|c_e|^2$ as in Ref. 8, which expresses directly the amount of exciton-cavity mixing in the polariton wave functions. Such a plot is shown in Fig. 5 for both polariton branches (lower branch, filled squares; upper branch, open squares). Low exciton fraction corresponds to low (high) temperature for the lower (upper) branch, whereas high exciton fraction corresponds to high (low) temperature for the lower (upper) branch. For clarity these temperature regimes are labeled on the figure.

The most notable result of Fig. 6 is the marked decrease of the lower polariton branch linewidth as $|c_e|^2$ increases towards resonance ($|c_e|^2 = 0.5$). Such a variation cannot be explained by transfer matrix simulations with the exciton treated as a Lorentz oscillator,⁸ nor by a convolution model of Gaussian (exciton) and Lorentzian (cavity) line shapes.¹²

By contrast a good fit to the lower branch linewidth variation is obtained from the motional narrowing model. The theoretical treatment is described in detail in Ref. 8, so we only summarize the key points here. Motional narrowing is a general term which is used to describe the reduction in width

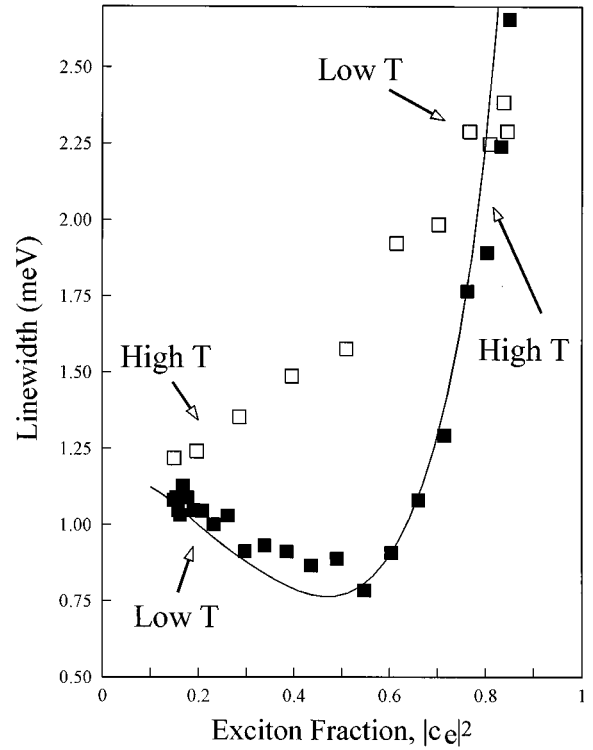


FIG. 5. Polariton linewidths as a function of exciton fraction $|c_e|^2$ for the upper branch (open squares) and the lower branch (filled squares). The fit to the motional narrowing model is given by the full line. Low T and high T indicate the temperature regimes from which the linewidth data are derived in the low and high $|c_e|^2$ limits.

of a spectral line in a disordered system by statistical averaging processes.¹³ In the microcavity, the motional narrowing arises because of the strong difference of the in-plane dispersion of curves of exciton-cavity polaritons compared to uncoupled, bare excitons.^{2,8,14} As discussed in Ref. 8, the cavity polaritons in the resonance regime have strong in-plane dispersion, with effective mass $\sim 10^{-5}m_0$. By contrast the uncoupled excitons have negligible dispersion and large mass at both zero and finite magnetic field (at $B=0$, the mass for in-plane exciton motion $M_{\text{ex}} = m_e + m_h \approx 0.2m_0$ where m_e and m_h are the electron and hole in-plane masses, and in finite magnetic field M_{ex} is infinite). It is the very small polariton effective mass which gives rise to the importance of motional narrowing in quantum microcavities.

Exciton linewidths in QW's are determined by the disorder potential (V_{dis}) in the quantum well arising from well width and alloy fluctuations.¹⁵ Due to its large in-plane mass the exciton is strongly localized in the disorder potential. The effective potential seen by the exciton is an average of V_{dis} over length scales of the order of the exciton Bohr radius of ~ 100 Å. Exciton linewidths of order of the width of the effective disorder potential are then expected. In the microcavity polariton case the effective mass is much smaller, the polariton wave function is much more extended, and strong averaging over the disorder potential is expected. As a result only a weak exciton disorder contribution to the coupled mode linewidth on resonance is expected, and motional narrowing results.

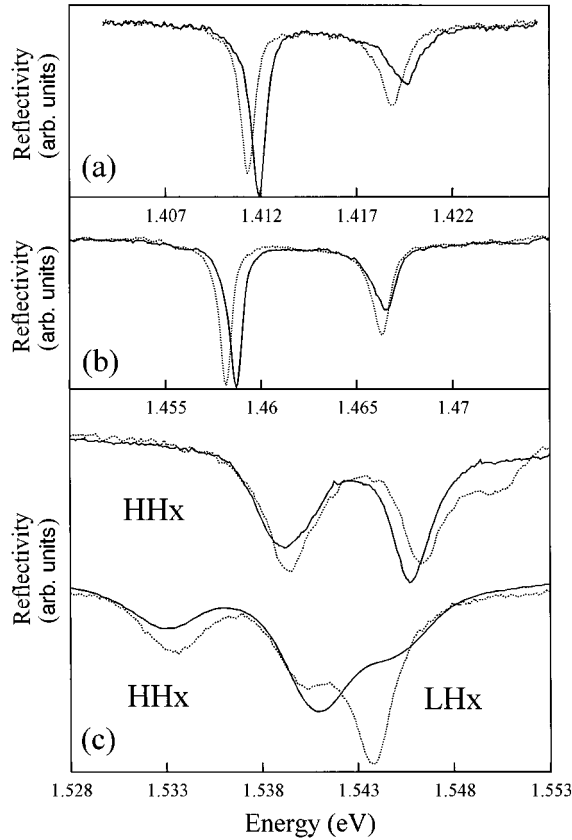


FIG. 6. Circularly polarized spectra at 14 T for microcavities with quantum wells of In composition $x=0.13$, 0.06 , and 0 . Full curves, σ^+ ; dashed curves, σ^- . For the $x=0$ GaAs QW structure both heavy-hole and light-hole spectra are shown. In all cases, the sample temperatures are varied to obtain near resonance spectra. The temperatures are 70 K ($x=0.13$), 80 K ($x=0.06$), and 80 K ($x=0$, HHx), 112 K ($x=0$, LHx). For $x=0.13$, $x=0.06$, and $x=0$ LHx, the σ^+ polarization lies at higher energy than σ^- corresponding to positive exciton g -values; for $x=0$ HHx σ^- lies at higher energy than σ^+ since the exciton g -value is negative.

The full line in Fig. 5 is the result of the predictions of the motional narrowing theory of Ref. 8. The disorder contribution to the linewidth is calculated as a function of $|c_e|^2$ and convolved with the cavity contribution $|c_l|^2\Gamma_l$, where $\Gamma_l = 1$ meV is the off-resonance cavity linewidth. As can be seen from Fig. 5, a very good fit to the linewidth variation of the lower branch versus $|c_e|^2$ is obtained. In particular the decreasing linewidth towards resonance, to a value below that of either of the two off-resonance widths, is reproduced very well. The agreement for the upper branch is, however, less good, possibly due to additional coupling to higher-energy exciton states.^{16,4}

We now discuss some additional points which arise from Fig. 5. It is notable that the linewidths for both the upper and lower branches agree very well in the limits of both low and high $|c_e|^2$. Since high $|c_e|^2$ corresponds to high and low temperature for the lower and upper branches, respectively, this shows that temperature-dependent broadening of the exciton linewidth is negligible as expected¹⁷ (at least up to 120 K), a fundamental assumption of our temperature tuning technique. Similar comments apply to the low $|c_e|^2$ limit which demonstrates negligible variation of the cavity line-

width with temperature, again as expected.

The good agreement between the cavity linewidths for both high and low temperature, corresponding to the exciton at lower and higher energy than the cavity, respectively, is particularly notable. Such a situation is not found at $B=0$ where marked broadening of the cavity peak is observed when the exciton peak is at lower energy than the cavity; absorption from exciton continuum states leads to a reduction of the finesse of the cavity and broadening of the cavity mode, as first commented on by Tignon *et al.*⁵ In high magnetic field the continuum states are quantized into discrete Landau levels, and such damping of the cavity mode no longer occurs; the cavity linewidths then agree well for the cases where the exciton is both at higher and lower energy than the cavity mode.

V. SPECTRA IN THE RESONANCE REGIME AS A FUNCTION OF QUANTUM-WELL INDIUM COMPOSITION

Near-resonance spectra at 14 T for three quantum microcavity samples containing quantum wells of composition $\text{In}_{0.13}\text{Ga}_{0.87}\text{As}$, $\text{In}_{0.06}\text{Ga}_{0.94}\text{As}$, and GaAs ($x=0.13$, 0.06 , and 0) are presented in Fig. 6 for σ^+ and σ^- polarizations. As discussed in Sec. III, exact resonance occurs at slightly different temperature for the two polarizations (by 12 K for the $x=0.13$ sample). The spectra shown in Fig. 6 are only exactly on-resonance for one of the two polarizations. The temperature for equal Zeeman splittings of the two branches corresponds to the average of the σ^+ and σ^- resonance temperatures. In the following, we label these equal Zeeman splittings ΔE_z .

The ΔE_z values corresponding to resonance with the heavy-hole excitons of the quantum wells for the three samples are 0.6 meV ($x=0.13$), 0.4 meV ($x=0.06$), and 0.36 meV ($x=0$), respectively, with σ^+ lying at higher energy than σ^- for $x=0.13$ and 0.06 and σ^- lying at higher energy for $x=0$. Using the two-level coupling model of Sec. III, and noting also that the ΔE_z values correspond to half the bare exciton Zeeman splittings,¹¹ we deduce exciton Zeeman splittings at 14 T of 1.2,¹⁸ 0.8, and 0.7 meV for the three samples.

Quantitative comparison with Zeeman splittings measured by other workers is difficult since effective exciton g values have been shown to be a sensitive function of well width,¹⁹ magnetic field,²⁰ and alloy composition.²⁰ This arises since the spin splitting of the lowest heavy-hole state (spin $m_j = \pm \frac{3}{2}$) is strongly affected by interaction with the lowest light-hole level,¹⁹ since only the $m_j = +\frac{3}{2}$ level interacts strongly with the light-hole states. These interactions act to reduce the expected heavy-hole spin splitting at energies where the heavy-hole state approaches the light-hole energy. Thus, in general, heavy-hole and hence exciton g values (g_{ex}) are expected to increase with increasing indium composition due to the increasing heavy-hole–light-hole splitting, as found in our experiments (1.2 meV at $x=0.13$, 0.8 meV at $x=0.06$), and to decrease with increasing magnetic field, since the heavy hole exhibits a larger diamagnetic shift than the light-hole state. Indeed, at high fields a sign reversal of the exciton g -value has been observed for samples of low or zero x having small heavy hole–light-hole splitting.^{19,20}

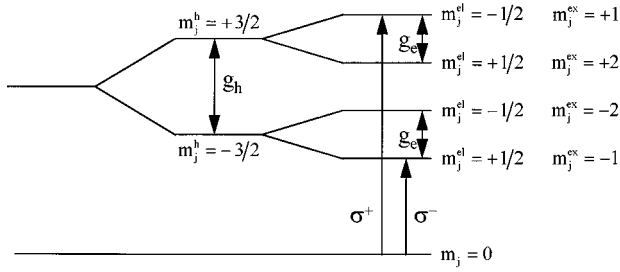


FIG. 7. Spin-splitting diagram showing origin of σ^+ and σ^- transitions for g_h large and positive ($x=0.13$, 0.06 samples) and g_e small and negative. m_j^h , m_j^e , and m_j^{ex} represent the magnetic quantum numbers m_j for the hole, electron, and exciton, respectively.

In light of the above we consider that the exciton Zeeman splitting we deduce of 1.2 meV at 14 T for the $x=0.13$ sample is in reasonable agreement with the most closely comparable result of 1.5 meV at 11 T for a quantum well with $x=0.1$ reported by Wimbauer *et al.*²¹ At $x=0.13$, the heavy-hole g value is expected to be large and positive ($g_h \approx 1$), and the electron g value small and negative. These signs of g values are employed in the schematic Zeeman splitting energy-level diagram shown in Fig. 7. The allowed $\Delta m_j = \pm 1$ (σ^+ , σ^-) transitions then arise from the outer two exciton spin components with the overall splitting of 1.1 meV at 14 T corresponding to $g_h + g_e = g_{\text{ex}} \approx 1.4$. As the indium composition is reduced, the hole g value is expected to become smaller with a consequent reduction in the exciton spin splitting, as found in the work of Traynor, Harley, and Warburton²⁰ and in our experiments.

At $x=0$ for the GaAs QW sample we observe a sign reversal of the polarization of the heavy-hole exciton reflectivity features, with σ^- lying at higher energy than σ^+ . This is in agreement with the high-field results of Snelling *et al.*¹⁹ discussed above, who found negative exciton g values for an 11 nm GaAs QW at fields greater than 3 T. Results are also shown in Fig. 7 for the $x=0$ sample at higher temperatures such that the light-hole exciton²² is on-resonance with the cavity. σ^+ now lies at higher energy than σ^- and shows an approximately 3 times greater splitting than the heavy hole, consistent with findings of, for example, Potemski *et al.*,²³ who report larger and oppositely polarized light-hole splittings relative to those observed for the heavy-hole ground state.

VI. TUNING OF HIGHER EXCITON STATES THROUGH THE CAVITY MODE

In magnetic field the exciton continuum states are quantized into Landau-level-like states. These discrete excitonic excited states can then interact with the cavity mode with a characteristic vacuum Rabi splitting on resonance. Such phenomena were first reported by Tignon *et al.* in Ref. 3. The variation of the first heavy-hole excitonic excited state transition energy, through the cavity mode energy, as a function of temperature, is shown in Fig. 8. The excited state transition, labeled $N=1$, tends towards the $N=1$ free-particle Landau-level transition energy in high magnetic field. Clear anticrossing behavior with the cavity mode is found, with

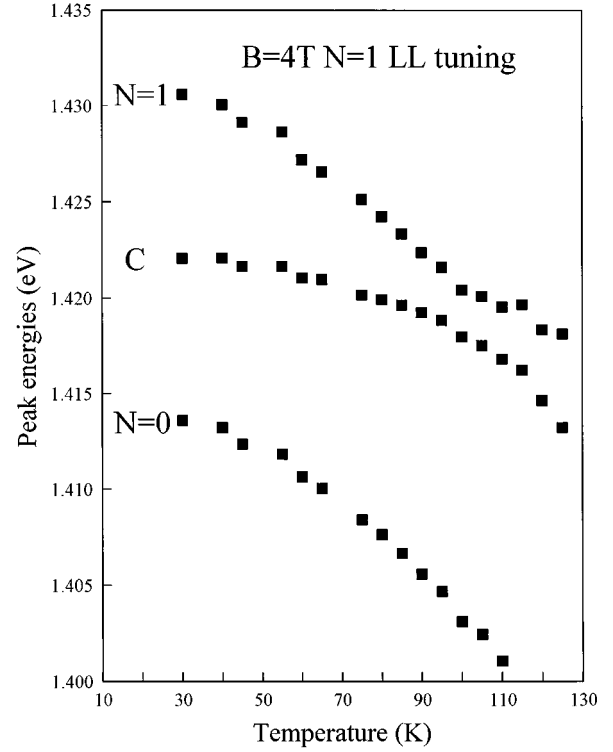


FIG. 8. Anticrossing tuning curves for the $N=1$ excitonic Landau-level transition at 4 T. Resonance is achieved at ~ 95 K. The transitions to lower energy arise from the $N=0$ exciton ground state. Data points are the average of the σ^- and σ^+ feature positions.

very similar overall form to that observed for the ground-state $N=0$ transition in Fig. 2. These experimental results were obtained on a different piece of the $x=0.13$ wafer from that employed for Figs. 1–6. The sample of Fig. 8 has cavity mode energy -8 meV at higher energy than the sample in Figs. 1–5, and shows resonance with the $N=1$ transition in an easily accessible temperature range.

On-resonance spectra for the $N=1$ excited state and $N=0$ ground-state transitions for the $x=0.13$ sample are presented in Figs. 9(a) and 9(b), respectively. The spectra of Fig. 9(a) are taken at 4 T with the temperature adjusted to 22 K to bring the $N=1$ peak and the cavity mode to resonance. For comparison, on-resonance spectra at 4 T from the excitonic ground state ($N=0$) are also shown in Fig. 9(b) for the sample of Figs. 1–5, in this case at a temperature of 98 K.

The vacuum Rabi splittings for the two cases are 2.5 meV ($N=1$) and 5.6 meV ($N=0$). Transfer matrix simulations were then performed to determine the relative oscillator strengths (f) of the transitions which control the size of the relative vacuum Rabi splittings. The resulting oscillator strengths were found to be in the ratio 1:3.3 ($N=1$ to $N=0$).²⁴ These ratios were then compared with the results of our quantum-well exciton calculations in magnetic field, which employ a numerical solution of Schrödinger's equation for a finite QW, with decoupled heavy- and light-hole bands. These calculations predict an oscillator strength ratio of 1:2.6 at 4 T in very reasonable agreement with the ratio deduced from the observed Rabi splittings.²⁵

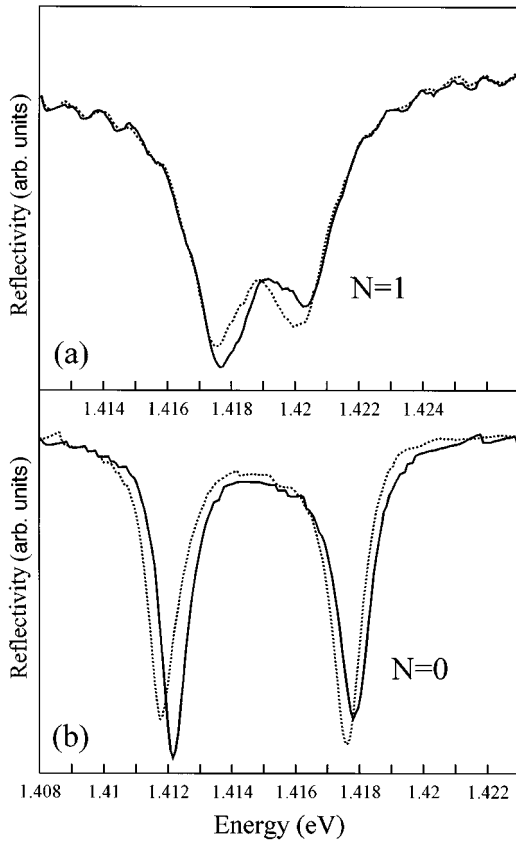


FIG. 9. Comparison of on-resonance magnetorefectivity at 4 T for (a) the $N=1$ exciton level transition and (b) the ground-state excitonic transition ($N=0$). The vacuum Rabi splitting in (a) is a factor of 2.2 smaller than in (b) as a result of the 3.3 times smaller oscillator strength of the $N=1$ transition. σ^+ polarization, full lines; σ^- polarization, dashed lines.

VII. CONCLUSIONS

The polariton spectra of high-quality quantum microcavity structures have been investigated in high magnetic field. Very-well-resolved spectra were observed as a result of the good sample quality and the enhancement of exciton oscillator strength in high magnetic field. Temperature tuning was employed at high magnetic field to vary the exciton and cavity fractions of the polariton spectra through the resonance regime in a controlled way. The exciton and cavity fractions of the polariton modes were then deduced by fitting the observed peak positions and on-resonance splitting to a two-level coupled-mode model.

The spectra were found to be strongly circularly polarized, with clear Zeeman splittings being observed. A very good fit to the variation of the observed Zeeman splittings

with detuning from resonance was found using the coupled mode model. Furthermore the on-resonance Zeeman splitting was found to be one-half the off-resonance value, as expected since on-resonance the polariton modes contain equal exciton and cavity fractions. The linewidths of the polariton modes through the resonance regime were also investigated. The lower polariton branch showed highly anomalous behavior, with observed linewidth on resonance being less than that of either the exciton or cavity modes off-resonance. This behavior was explained by a motional narrowing theory for polariton linewidths in a microcavity. A very good fit to the variation of the lower branch polariton linewidth as a function of detuning was obtained. The fit to the upper branch was however found to be less good, probably due to coupling of this branch to higher-order exciton states, not included in the theoretical treatment. The advantages of performing such tuning experiments in high magnetic field were emphasized. In particular, the quantization of exciton continuum states in magnetic field was shown to lead to nearly equal cavity mode linewidths for the exciton mode occurring either to higher or lower energy than the cavity mode. This situation contrasts strongly with that found at zero magnetic field where the cavity mode is found to be strongly broadened when the exciton peak is to lower energy, due to absorption by exciton continuum states at the cavity mode energy.

The Zeeman splittings were also investigated as a function of indium composition (x) in the quantum wells. A decrease of Zeeman splitting was found with decreasing x , due to the decrease of hole g value with decreasing x , in agreement with previous results for exciton spin splittings in bare quantum-well samples. For GaAs quantum wells in the microcavities, Zeeman splittings of opposite sign were observed, again consistent with previous work on quantum wells. The good qualitative agreement between the exciton Zeeman splittings deduced from the microcavity spectra, over a range of x values, and those reported for bare QW's provides additional confirmation of the correctness of the analysis of the microcavity polariton spectra in high magnetic field. Finally, coupling of the first magnetoexciton excited state transition ($N=1$) with the cavity mode was investigated. Significantly smaller vacuum Rabi splittings than for the $N=0$ ground state were observed, due to the smaller oscillator strength for the $N=1$ transition. The ratio of the observed vacuum Rabi splitting for $N=1$ to that found for $N=0$ was found to be in good agreement with the results of quantum-well magnetoexciton calculations.

ACKNOWLEDGMENTS

We would like to thank R. T. Harley, N. J. Traynor, and A. J. Shields for very helpful discussions of exciton spin splittings in quantum wells.

*Present address: Toshiba Cambridge Research Centre, Cambridge Science Park, Milton Road, Cambridge CB4 4WE, UK.

¹C. Weisbuch, M. Nishioka, A. Ishikawa, and Y. Arakawa, *Phys. Rev. Lett.* **69**, 3314 (1992).

²R. Houdre, C. Weisbuch, R. P. Stanley, U. Oesterle, P. Pellandini, and M. Ilegems, *Phys. Rev. Lett.* **73**, 2048 (1994).

³J. Tignon, P. Voison, C. Delalande, M. Voos, R. Houdre, U. Oesterle, and R. P. Stanley, *Phys. Rev. Lett.* **74**, 3967 (1995).

⁴T. A. Fisher, A. M. Afshar, M. S. Skolnick, D. M. Whittaker, and J. S. Roberts, *Phys. Rev. B* **53**, R10 469 (1996).

⁵J. D. Berger, O. Lyngnes, H. M. Gibbs, G. Khitrova, T. R. Nelson, E. K. Lindmark, A. V. Kavokin, M. A. Kaliteevski, and V. V. Zapasski, *Phys. Rev. B* **54**, 1975 (1996).

⁶T. A. Fisher, A. M. Afshar, D. M. Whittaker, M. S. Skolnick, J. S. Roberts, G. Hill, and M. A. Pate, *Phys. Rev. B* **51**, 2600 (1995).

⁷T. A. Fisher, A. M. Afshar, M. S. Skolnick, D. M. Whittaker, J. S.

- Roberts, G. Hill, and M. A. Pate, *Solid-State Electron.* **40**, 493 (1996).
- ⁸D. M. Whittaker, P. Kinsler, T. A. Fisher, M. S. Skolnick, A. Armitage, A. M. Afshar, and J. S. Roberts, *Phys. Rev. Lett.* **77**, 4792 (1996).
- ⁹The algebraic expressions for c_e and c_l obtained from the diagonalization for one branch are $c_e = \sqrt{(\delta + \Delta)/2\delta}$ and $c_l = \sqrt{(\delta - \Delta)/2\delta}$. Similar expressions can be found in B. Sermage *et al.*, *Phys. Rev. B* **53**, 16 516 (1996).
- ¹⁰The temperature for equal Zeeman splittings of 75 K agrees well with the average resonance temperature for the σ^+ and σ^- polarizations of 76 K (average of 82 and 70 K). This good agreement provides support for the identification of resonance as corresponding to equal integrated areas of the two polariton branches as discussed in Sec. III A. In Ref. 4, resonance was taken to correspond to equal peak depth of the two polariton branches in unpolarized spectra, thus leading to a small overestimate (by ~ 5 K) of the resonance temperatures. This also results in unequal Zeeman splittings of the two polariton branches at resonance, in disagreement with the two-level model.
- ¹¹Further discussion of the point is given in Ref. 16 of Ref. 4, where degenerate perturbation theory arguments are used to show that the on-resonance Zeeman splitting is one half of the off-resonance value, to a very good approximation.
- ¹²P. Kinsler and D. M. Whittaker, *Phys. Rev. B* **54**, 4988 (1996).
- ¹³See, for example, A. Abragam, *The Principles of Nuclear Magnetism* (Clarendon, Oxford, 1961), p. 446.
- ¹⁴S. Pau, G. Bjork, J. Jacobsen, H. Cao, and Y. Yamamoto, *Phys. Rev. B* **51**, 7090 (1995).
- ¹⁵J. Singh and K. K. Bajaj, *Appl. Phys. Lett.* **48**, 1077 (1986).
- ¹⁶R. Houdre, R. P. Stanley, U. Oesterle, M. Ilegems, and C. Weisbuch, *Phys. Rev. B* **49**, 16 761 (1994).
- ¹⁷D. S. Chemla, D. A. B. Miller, P. W. Smith, A. C. Gossard, and W. Wiegmann, *IEEE J. Quantum Electron.* **20**, 265 (1984).
- ¹⁸In our previous publication on magnetic field studies of the $x = 0.13$ sample, resonance was taken as equal peak depth for the upper and lower polariton peaks (see Ref. 10). As a result this corresponded to a larger Zeeman splitting for the lower polariton peak, with the splitting being unresolved on the upper peak. This accounts for the larger exciton Zeeman splitting of 1.7 meV at 14 T in Ref. 4 than the 1.1 meV reported here.
- ¹⁹M. J. Snelling, G. P. Flinn, A. S. Plaut, R. T. Harley, A. C. Tropper, R. Eccleston, and C. C. Phillips, *Phys. Rev. B* **44**, 11 345 (1991).
- ²⁰N. J. Traynor, R. T. Harley, and R. J. Warburton, *Phys. Rev. B* **51**, 7361 (1995).
- ²¹Th. Wimbauer, K. Oettinger, A. L. Efros, and B. K. Meyer, *Phys. Rev. B* **50**, 8889 (1994).
- ²²Light-hole resonances are not observed for the samples with finite indium composition, since the light-hole levels are shifted strongly to higher energy by the strain in the samples.
- ²³M. Potemski, J. C. Maan, A. Fasolino, K. Ploog, and G. Weimann, *Phys. Rev. Lett.* **63**, 2409 (1989).
- ²⁴The vacuum Rabi splittings are only accurately proportional to the square root of exciton oscillator strength when the polariton linewidths are significantly less than the splittings between the branches. This limit is not reached for the $N=1$ Landau-level crossing. As a result the oscillator strength ratio of 3.3 obtained from the TMR fit is reduced below the value of $(5.6/2.5)^2 = 5.0$ that would be obtained from the square of the on-resonance splittings, see, e.g., Y. Zhu *et al.* *Phys. Rev. Lett.* **64**, 2499 (1990). Physically, the $N=1$ oscillator strength is significantly smaller than that for $N=0$ due to the more extended nature of the $N=1$ wave function.
- ²⁵The input parameters for the calculation are given in Ref. 13 of Ref. 4.